Published for SISSA by Springer

Received: December 28, 2016
Revised: April 26, 2017
Accepted: May 9, 2017
Published: May 31, 2017

JHEP05(2017)158

Search for the $B_s^0 \to \eta'\phi$ decay

The LHCb collaboration

E-mail: sebastiana.giani@epfl.ch

Abstract: A search for the charmless $B_s^0 \to \eta'\phi$ decay is performed using pp collision data collected by the LHCb experiment at centre-of-mass energies of 7 and 8 TeV, corresponding to an integrated luminosity of $3\,\text{fb}^{-1}$. No signal is observed and upper limits on the $B_s^0 \to \eta'\phi$ branching fraction are set to 0.82×10^{-6} at 90% and 1.01×10^{-6} at 95% confidence level.

Keywords: B physics, Branching fraction, Hadron-Hadron scattering (experiments)

ArXiv ePrint: 1612.08110

doi:10.1007/JHEP05(2017)158

Contents

JHEP05(2017)158

1 Introduction

Charmless hadronic decays of beauty hadrons proceed predominantly through tree-level $b \to u$ and loop-level (penguin) $b \to s$ weak transitions. In the Standard Model the amplitudes of these processes, suppressed compared to the dominant tree $b \to c$ transition governing charmed decays, usually have similar magnitudes and give rise to possibly large violation of the charge-parity (CP) symmetry. Therefore, charmless decays of B mesons should be sensitive to additional amplitudes from new, heavy particles, contributing to the loop-level transitions [1].

Charmless hadronic B^+ and B^0 decays[1] have been the subject of extensive studies, both experimentally, at hadron and e^+e^- colliders, and theoretically. The phenomenological understanding that has emerged allows predictions to be made for charmless B_s^0 decays, as will be illustrated in the following. In the ongoing effort to test these predictions experimentally, the LHCb experiment has recently observed the decay[2] $B_s^0 \to \eta'\eta'$. The relatively large measured branching fraction $\mathcal{B}(B_s^0 \to \eta'\eta') = (33.1 \pm 7.1) \times 10^{-6}$ is consistent with Standard Model expectations [2]. However, the knowledge about charmless hadronic B_s^0 decays into light pseudoscalar (P) and vector (V) mesons is still limited. Further measurements will help to better constrain phenomenological models, the uncertainties of which often translate into a major contribution to the theoretical uncertainties in searches for physics beyond the Standard Model.

The decay $B_s^0 \to \eta'\phi$ proceeds predominantly through $\bar{b} \to \bar{s}s\bar{s}$ transitions, as illustrated in figure 1. It is of particular interest in constraining phenomenological models, as predictions for its branching fraction cover a wide range, typically from 0.1×10^{-6} to 20×10^{-6}, with large uncertainties that reflect the limited knowledge of form factors, penguin contributions, the $\omega - \phi$ mixing angle, or the s-quark mass. The decay $B_s^0 \to \eta'\phi$ has been studied

[1] The inclusion of charge-conjugate processes is implied throughout.

[2] The notations η' and ϕ refer to the $\eta'(958)$ and $\phi(1020)$ mesons.

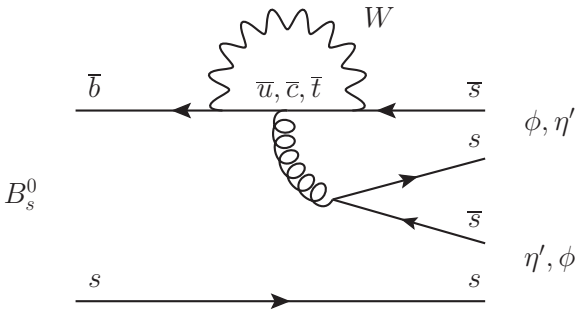

Figure 1. Lowest-order diagrams for the $B_s^0 \to \eta'\phi$ decay. The spectator quark can become part of either the η' or the ϕ meson, forming two different amplitudes (called PV and VP in the text).

in the framework of QCD factorisation [3, 4], perturbative QCD [5, 6], soft-collinear effective theory (SCET) [7], SU(3) flavour symmetry [8], and factorisation-assisted topological (FAT) amplitude approach [9]. Table 1 presents the available predictions for $\mathcal{B}(B_s^0 \to \eta'\phi)$.

In QCD factorisation, predictions for $\mathcal{B}(B_s^0 \to \eta'\phi)$ are generally small because the spectator quark can become part of either the η' or the ϕ meson (see figure 1), leading to a strong cancellation between the PV and VP amplitudes contributing to the $\eta'\phi$ final state [3]. Such cancellation does not occur in the symmetric $B_s^0 \to \eta'\eta'$ (PP) and $B_s^0 \to \phi\phi$ (VV) decays. However, other values of the form factor for the B_s^0 to ϕ transitions can lead to enhancements of the branching fraction by more than an order of magnitude [4]. The measurement of $\mathcal{B}(B_s^0 \to \eta'\phi)$ is therefore important to improve the knowledge of the B_s^0 to ϕ form factor and the accuracy of model predictions.

The comparison of QCD factorisation [3, 4], perturbative QCD [5], and SCET [7] calculations shows that the hierarchy of branching fractions in $B_s^0 \to \eta'\phi$ and $B_s^0 \to \eta\phi$ decays is sensitive to the size of the colour-suppressed QCD penguin loop, which is estimated to be large in perturbative QCD [5], and to "gluonic charming penguins", which play an important role in SCET calculations [7]. Future measurements of both decay modes will provide useful information on these loop contributions.

This paper presents a search for the $B_s^0 \to \eta'\phi$ decay with the LHCb detector. The results are based on a data sample collected during the 2011 and 2012 pp collision runs of the Large Hadron Collider at centre-of-mass energies of 7 and 8 TeV, respectively, corresponding to a total integrated luminosity of $3\,\text{fb}^{-1}$.

The signal $B_s^0 \to \eta'\phi$ and normalisation $B^+ \to \eta' K^+$ candidates are reconstructed through the decays $\eta' \to \pi^+\pi^-\gamma$ and $\phi \to K^+K^-$. The $B_s^0 \to \eta'\phi$ branching fraction is determined with respect to the $B^+ \to \eta' K^+$ mode according to

$$\mathcal{B}(B_s^0 \to \eta'\phi) = \frac{\mathcal{B}(B^+ \to \eta' K^+)}{\mathcal{B}(\phi \to K^+K^-)} \times \frac{f_u}{f_s} \times \frac{N(B_s^0 \to \eta'\phi)}{N(B^+ \to \eta' K^+)} \times \frac{\epsilon(B^+ \to \eta' K^+)}{\epsilon(B_s^0 \to \eta'\phi)}\,, \tag{1.1}$$

where $\mathcal{B}(B^+ \to \eta' K^+) = (70.6 \pm 2.5) \times 10^{-6}$ [10], $\mathcal{B}(\phi \to K^+K^-) = 0.489 \pm 0.005$ [10], f_u/f_s is the B^+/B_s^0 production ratio assumed to be equal to the B^0/B_s^0 production ratio $f_d/f_s = 1/(0.259 \pm 0.015)$ [11, 12], and $\epsilon(B_s^0 \to \eta'\phi)$ and $\epsilon(B^+ \to \eta' K^+)$ are the total efficiencies of the signal and normalisation modes, respectively. The ratio of the observed

JHEP05(2017)158

Theory approach	$\mathcal{B}$ (10^{-6})	Reference
QCD factorisation	$0.05^{+1.18}_{-0.19}$	[3]
QCD factorisation	$2.2^{+9.4}_{-3.1}$	[4]
Perturbative QCD	$0.19^{+0.20}_{-0.13}$	[5]
Perturbative QCD	$20.0^{+16.3}_{-9.1}$	[6]
SCET	$4.3^{+5.2}_{-3.6}$	[7]
SU(3) flavour symmetry	5.5 ± 1.8	[8]
FAT	13.0 ± 1.6	[9]

Table 1. Theoretical predictions for the $B^0_s \to \eta'\phi$ branching fraction.

yields $N(B^0_s \to \eta'\phi)/N(B^+ \to \eta' K^+)$ is obtained from a two-dimensional fit to the invariant mass distributions of the η' and the B candidates, performed simultaneously on the signal and normalisation modes.

2 Detector and simulation

The LHCb detector [13, 14] is a single-arm forward spectrometer covering the pseudorapidity range $2 < \eta < 5$, designed for the study of particles containing b or c quarks. The detector includes a high-precision tracking system consisting of a silicon-strip vertex detector surrounding the pp interaction region, a large-area silicon-strip detector located upstream of a dipole magnet with a bending power of about 4 Tm, and three stations of silicon-strip detectors and straw drift tubes placed downstream of the magnet. The tracking system provides a measurement of momentum of charged particles with a relative uncertainty that varies from 0.5% at low momentum to 1.0% at 200 GeV/c. The minimum distance of a track to a pp-collision point (primary vertex), the impact parameter, is measured with a resolution of $(15 + 29/p_{\rm T})\,\mu$m, where $p_{\rm T}$ is the component of the momentum transverse to the beam, in GeV/c. Different types of charged hadrons are distinguished using information from two ring-imaging Cherenkov detectors. Photons, electrons and hadrons are identified by a calorimeter system consisting of scintillating-pad (SPD) and preshower detectors, an electromagnetic calorimeter and a hadronic calorimeter. Muons are identified by a system composed of alternating layers of iron and multiwire proportional chambers.

The trigger [15] consists of a hardware stage, based on information from the calorimeter and muon systems, followed by a software stage, which applies a full event reconstruction. The B decays of interest are triggered at the hardware stage, either by one of the decay products depositing a transverse energy greater than 3.5 GeV in the hadron calorimeter, or by other high-$p_{\rm T}$ particles produced in the pp collision. The software trigger requires a two-, three- or four-track secondary vertex with a significant displacement from the primary vertices. At least one charged particle must have a transverse momentum $p_{\rm T} > 1.7$ GeV/c

JHEP05(2017)158

and be inconsistent with originating from a primary vertex. A multivariate algorithm [16] is used for the identification of secondary vertices consistent with the decay of a b hadron.

Simulated decays are used to optimise the event selection and to evaluate the selection efficiencies. In the simulation, pp collisions are generated using Pythia 8 [17, 18] with a specific LHCb configuration [19]. Decays of hadronic particles are described by EvtGen [20], in which final-state radiation is generated using Photos [21]. The interaction of the generated particles with the detector, and its response, are implemented using the Geant4 toolkit [22, 23] as described in ref. [24].

3 Event selection

The selection of the signal $B_s^0 \to \eta'\phi$ and normalisation $B^+ \to \eta' K^+$ candidates, generically referred to as B candidates, is optimised for the signal. Wherever possible, the same selection criteria are applied for the normalisation channel.

Only good-quality tracks identified as pions or kaons [14] and inconsistent with originating from any primary vertex are used. Tracks used to reconstruct an η' or ϕ candidate are each required to be consistent with coming from a common secondary vertex and to have $p_{\rm T} > 0.4\,{\rm GeV}/c$. The $\pi^+\pi^-$ invariant mass in the η' decay must be larger than $0.52\,{\rm GeV}/c^2$ to reject $K^0_{\rm S} \to \pi^+\pi^-$ decays. Photon candidates must be of good quality [14] and have $p_{\rm T} > 0.3\,{\rm GeV}/c$. The invariant masses of the η' and ϕ candidates must satisfy $0.88 < m_{\pi\pi\gamma} < 1.04\,{\rm GeV}/c^2$ and $1.005 < m_{KK} < 1.035\,{\rm GeV}/c^2$. An η' candidate is combined with a candidate ϕ meson (or a charged kaon with $p_{\rm T} > 1\,{\rm GeV}/c$) to make a B_s^0 (or B^+) candidate. Each B candidate is required to have a good-quality vertex, by imposing a loose requirement of the χ^2 of the vertex fit ($\chi^2 < 6$), and $p_{\rm T} > 1.5\,{\rm GeV}/c$. The invariant masses of the B_s^0 and B^+ candidates, computed after constraining the $\pi^+\pi^-\gamma$ mass to the nominal η' mass [10], are required to satisfy $5.0 < m_{\eta' KK} < 5.6\,{\rm GeV}/c^2$ and $5.0 < m_{\eta' K} < 5.5\,{\rm GeV}/c^2$, respectively.

To further separate signal from background, boosted decision trees (BDTs) based on the AdaBoost algorithm [25, 26] are used. Different BDTs are used for the signal and normalisation channels. Each BDT is trained, tested and optimised on fully simulated signal decays and background taken from data. The background consist of events in the mass range $5.0 < m_{\eta' KK} < 5.6\,{\rm GeV}/c^2$ ($5.0 < m_{\eta' K} < 5.5\,{\rm GeV}/c^2$) excluding the signal region defined below.

To minimise statistical and systematic uncertainties, the BDT algorithm uses input variables that provide significant background rejection, are well modelled in simulation, and are defined for both the signal and normalisation channels. Nine variables are used as input to each BDT. Two variables are related to the kinematics of the final-state particles: the transverse momenta of the photon and the η' meson. Three variables describe the topology of the B candidate: the B-candidate flight distance, the cosine of the angle between the reconstructed B momentum and the vector pointing from the associated primary vertex to the B decay vertex, and the impact parameter of the B candidate with respect to its associated primary vertex. The associated primary vertex is the primary vertex with respect to which the B candidate has the smallest $\chi^2_{\rm IP}$, where $\chi^2_{\rm IP}$ is defined

JHEP05(2017)158

as the difference in the vertex-fit χ^2 of the selected primary vertex reconstructed with or without the considered particle. Three variables are related to the B-candidate vertex: the vertex-fit quality, characterised by its χ^2, and two vertex isolation variables defined as the smallest vertex-fit χ^2 values obtained when adding to the vertex in turn either all single tracks or all pairs of tracks from the set of tracks that are not assigned to the B candidate. The last variable is the sum of the $\chi^2_{\rm IP}$ of the charged particles used to form the B candidate, calculated with respect to the associated primary vertex. The photon $p_{\rm T}$ and the B-candidate impact parameter provide the best background discrimination. The BDT is trained for the full data set, irrespective of the pp collision energy. To minimise biases in the final selection, both the data and simulated samples are randomly divided into two subsamples and two BDTs are defined. Each BDT is trained, tested and optimised on one subsample, and then applied to the other subsample for the candidate selection [27]. The selected candidates from both subsamples are then merged into a single sample for the next stage of the analysis.

The requirement on the BDT output is chosen to maximise the figure of merit $\epsilon(B^0_s \to \eta'\phi)/(a/2 + \sqrt{N_B})$ [28], where $a = 5$ is the target signal significance, and N_B is the number of background events in the signal region estimated from the B^0_s mass sidebands. The signal region is defined as the B^0_s mass range 5.287–5.446 GeV/c^2, corresponding approximately to 7 times the mass resolution. The optimised BDT requirement has an efficiency of 59% for $B^0_s \to \eta'\phi$ decays, while rejecting 93% of the combinatorial background in the signal region. As a check, an alternative optimisation is performed: for various values of the $B^0_s \to \eta'\phi$ branching fraction, pseudoexperiments are generated with a model containing only signal and combinatorial background, and then are analysed with a simple two-dimensional maximum likelihood fit to the B^0_s and η' masses. The signal significance, determined using Wilks' theorem [29], is found to reach its maximum for a BDT requirement in agreement with that obtained using the method of ref. [28].

In events containing multiple candidates ($\lesssim 3\%$), the candidate with the best identified photon is kept. The full selection described above retains 430 $B^0_s \to \eta'\phi$ candidates and 22 681 $B^+ \to \eta' K^+$ candidates for further analysis.

Selection efficiencies are evaluated with simulated data, except those of the particle identification (PID) requirements and the hardware trigger, for which calibration data are used. Systematic uncertainties on the efficiency ratio $\epsilon(B^+ \to \eta' K^+)/\epsilon(B^0_s \to \eta'\phi)$ are summarised in table 2. The BDT algorithms are validated using the normalisation channel as proxy for the signal, and by comparing the distributions obtained with the *sPlot* technique [30] of the nine input variables and the BDT output variable. The difference between the efficiencies in data and simulation of the BDT requirement for the normalisation channel is used as a measure of the systematic uncertainty on the BDT efficiency. The correlation evaluated in simulation between the BDT variables for $B^0_s \to \eta'\phi$ and $B^+ \to \eta' K^+$ is then used to determine the systematic uncertainty on the ratio of the BDT efficiencies.

Another systematic effect on the determination of the efficiency ratio is the uncertainty on the PID efficiency, which is determined as a function of kinematic parameters using a clean high-statistics sample of kaons and pions from $D^{*+} \to D^0(\to K^-\pi^+)\pi^+$ decays [31]. The uncertainty on the trigger efficiency, which is mostly due to the computation of the

JHEP05(2017)158

Source	Relative uncertainty [%]
BDT efficiency calibration	2.5
PID efficiency calibration	1.1
Trigger efficiency calibration	2.3
SPD multiplicity (mismodelling)	0.9
Track reconstruction	0.4
Photon reconstruction	0.1
Hadronic interactions	1.4
Simulation statistics	1.6
Total	4.3

Table 2. Relative systematic uncertainties on the efficiency ratio $\epsilon(B^+ \to \eta' K^+)/\epsilon(B_s^0 \to \eta'\phi)$.

hardware-stage trigger efficiency, is estimated with simulated data by varying the value of the minimum transverse energy requirement used in the trigger decision. An uncertainty is assigned on the efficiency ratio to take into account the mismodelling of the hit multiplicity in the SPD, which is used as a discriminant variable at the hardware stage of the trigger. This uncertainty is evaluated in simulation by varying the requirement on the SPD hit multiplicity. Corrections determined from control channels are applied to the tracking and photon reconstruction efficiencies to account for mismodelling effects in the simulation. The uncertainties on these corrections are quoted as systematic uncertainties. Since the correction to the tracking efficiency is obtained using muons, an additional uncertainty is needed to account for hadronic interactions in the detector material [32]. Finally, the limited statistics of the simulated samples used in the evaluation of the efficiencies is added as a source of uncertainty. Combining all uncertainties in quadrature, the ratio of the selection efficiencies is

$$\frac{\epsilon(B^+ \to \eta' K^+)}{\epsilon(B_s^0 \to \eta'\phi)} = 1.83 \pm 0.08\,. \tag{3.1}$$

The selection requirements efficiently reject physics backgrounds such as $B^0 \to \phi K^{*0}$ and modes with resonances decaying strongly to $K^+\pi^-\pi^0$, but not $B_s^0 \to \phi\phi$ decays with one of the two ϕ resonances decaying to $\pi^+\pi^-\pi^0$ and one of the photons from the $\pi^0 \to \gamma\gamma$ decay not being reconstructed. From simulation studies and known branching fractions [10], the number of $B_s^0 \to \phi\phi$ decays passing the selection is expected to be 104 ± 34. Hence this background is included as a specific component in the mass fit described below.

4 Mass fit

The $B_s^0 \to \eta'\phi$ signal yield is determined from a two-dimensional extended unbinned maximum likelihood fit, where the signal is fitted simultaneously with the normalisation channel $B^+ \to \eta' K^+$. The observables used in the fit are the invariant masses $m_{\pi\pi\gamma}$ and $m_{\eta' KK}$ ($m_{\eta' K}$) for the sample of $B_s^0 \to \eta'\phi$ ($B^+ \to \eta' K^+$) candidates.

JHEP05(2017)158

The sample of $B_s^0 \to \eta'\phi$ candidates is described with a four-component model: the signal, the two combinatorial backgrounds with and without a true η' resonance, and the $B_s^0 \to \phi\phi$ physics background, where one of the two ϕ resonances decays to the $\pi^+\pi^-\pi^0$ final state. The sample of $B^+ \to \eta' K^+$ candidates is modelled using three components: the signal and the two combinatorial backgrounds with and without a true η' resonance. The yields of all components are free to vary in the fit. The peaking components in the B_s^0, B^+ and η' mass spectra are described using Gaussian functions modified with an exponential tail on each side. While all the tail parameters are fixed from simulation, the mean and the widths of the Gaussian functions are free to vary in the fit, but the ratio of the widths of the peaking components in $m_{\eta' KK}$ and $m_{\eta' K}$ is fixed to the value obtained in simulation and the difference between the B_s^0 and B^+ masses is constrained to the known value [10]. The η' resonances in the two samples are modelled using a common function, with mean and width free in the fit. The combinatorial components are described with linear functions, with the exception of the random combinations in $m_{\eta' K}$, where a parabolic function is used. To account for correlations between $m_{\eta' KK}$ and $m_{\pi\pi\gamma}$, the $B_s^0 \to \phi\phi$ component is described with a superposition of two-dimensional Gaussian kernel functions [33] determined from simulation. For all other components, in particular the signal, the correlation is negligible due to the η' mass constraint applied in the computation of the B-candidate mass. The fit procedure is validated on simulated samples containing the expected proportion of background and signal events, according to various assumptions on $\mathcal{B}(B_s^0 \to \eta'\phi)$. In particular, for $\mathcal{B}(B_s^0 \to \eta'\phi) = 4 \times 10^{-6}$, a statistical significance corresponding to more than 5 standard deviations is observed in 74% of the pseudoexperiments.

Figure 2 shows the mass distributions observed in data with the projections of the fit results overlaid. No $B_s^0 \to \eta'\phi$ signal is observed. The fitted yields are $-3.2^{+5.0}_{-3.8}$ for the $B_s^0 \to \eta'\phi$ signal, 105 ± 29 for the $B_s^0 \to \phi\phi$ physics background (consistent with expectation), and $11\,081 \pm 127$ for the $B^+ \to \eta' K^+$ normalisation mode. The measured B and η' mass resolutions are $21.8 \pm 0.3\,\mathrm{MeV}/c^2$ and $12.6 \pm 0.2\,\mathrm{MeV}/c^2$, respectively. The ratio of yields is fitted to be $N(B_s^0 \to \eta'\phi)/N(B^+ \to \eta' K^+) = (-2.9^{+4.5}_{-3.5}) \times 10^{-4}$.

Sets of pseudoexperiments are used to evaluate possible fit biases. Fits on samples generated from the probability density function (PDF) with parameters obtained from the data are found to be unbiased. The procedure is then repeated using simulated $B_s^0 \to \phi\phi$ events instead of generating the corresponding background component from the PDF. Biases of -1.3 ± 0.3 on the signal yield and of $(-1.16 \pm 0.33) \times 10^{-4}$ on the ratio of yields are observed. The results obtained with data are corrected for these biases and systematic uncertainties computed as the quadratic sum of the statistical uncertainty on the bias and half of the bias value are assigned.

Additional systematic uncertainties affect the signal yield and the yield ratio. The mass fit is repeated with different combinatorial background PDFs: linear functions are replaced with exponential functions, and the parabolic function is replaced with a third-order polynomial. The quadratic sum of the differences between the values obtained in these alternative fits and the nominal result is assigned as a systematic uncertainty. The limited size of the simulated $B_s^0 \to \phi\phi$ sample leads to an uncertainty on the determination of

JHEP05(2017)158

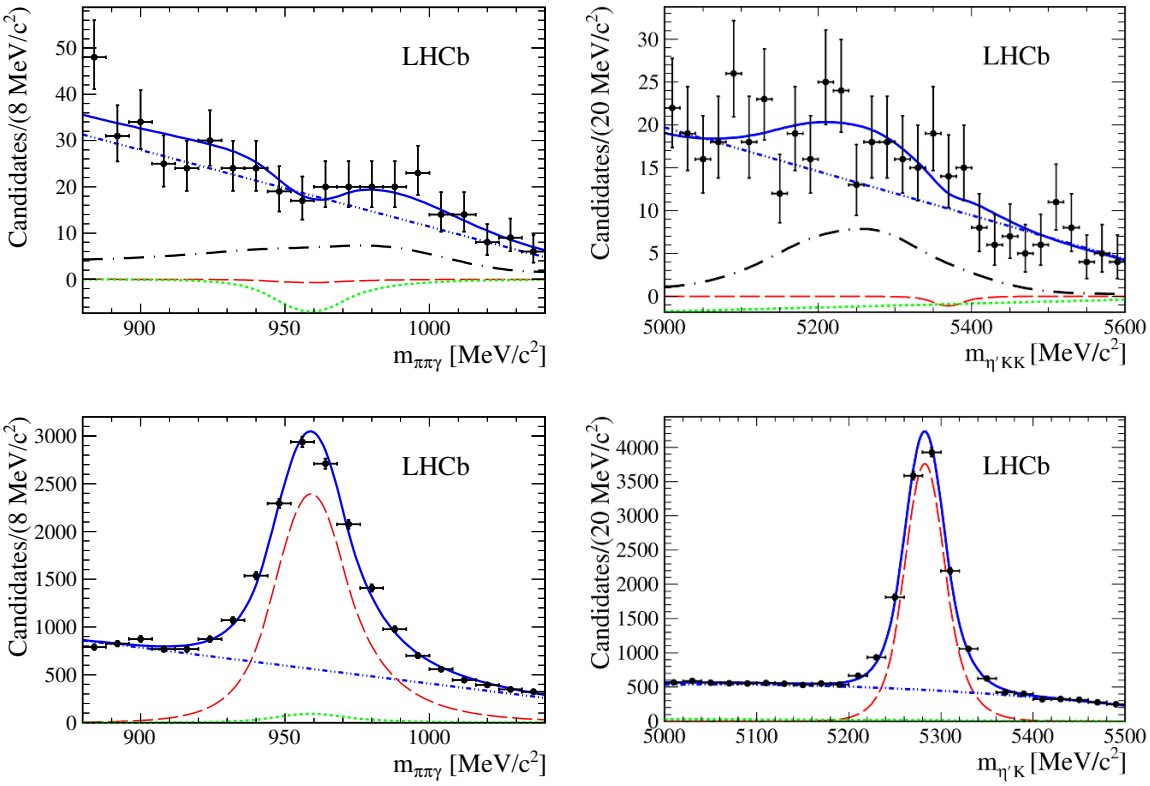

Figure 2. Distributions of the (top left) $\pi^+\pi^-\gamma$ and (top right) $\eta' K^+K^-$ masses of the selected $B_s^0 \to \eta'\phi$ candidates, as well as of the (bottom left) $\pi^+\pi^-\gamma$ and (bottom right) $\eta' K^+$ masses of the selected $B^+ \to \eta' K^+$ candidates. The solid blue curves represent the result of the simultaneous two-dimensional fit described in the text, with the following components: $B_s^0 \to \eta'\phi$ and $B^+ \to \eta' K^+$ signals (red dashed), combinatorial backgrounds (blue dot-dot-dashed), combinatorial backgrounds with real η' (green dotted), and $B_s^0 \to \phi\phi$ background (black dot-dashed).

the nonparametric PDF for the physics background, which is propagated as a systematic uncertainty. The effect of fixing some of the model parameters in the fit is studied by performing a large number of fits on the data, with the fixed parameters sampled randomly from Gaussian distributions centred on the nominal values and with widths and correlations as determined in simulated events. The standard deviation of the distribution of the results is assigned as a systematic uncertainty.

The systematic uncertainties on the $B_s^0 \to \eta'\phi$ yield and the yield ratio are summarised in table 3. The final results from the mass fit, including all corrections, are

$$N(B_s^0 \to \eta'\phi) = -1.9^{+5.0}_{-3.8} \pm 1.1\,, \tag{4.1}$$

$$\frac{N(B_s^0 \to \eta'\phi)}{N(B^+ \to \eta' K^+)} = (-1.7^{+4.5}_{-3.5} \pm 1.0) \times 10^{-4}\,, \tag{4.2}$$

where the first (second) quoted uncertainty is statistical (systematic). Bayesian upper limits $x_{\rm U}$ are determined assuming a uniform prior in the observable x (yield, yield ratio, or $\mathcal{B}$) as $\int_0^{x_{\rm U}} \mathcal{L}(x)dx / \int_0^{\infty} \mathcal{L}(x)dx = \alpha$, where $\mathcal{L}(x)$ is the likelihood function convolved

JHEP05(2017)158

Source	σ_N (events)	σ_R (10^{-4})
Fit bias	0.7	0.7
Combinatorial background modelling	0.6	0.6
$B_s^0 \to \phi\phi$ background modelling	0.4	0.3
Fixed parameters in the fit	0.3	0.3
Total	1.1	1.0

Table 3. Systematic uncertainties σ_N and σ_R on the fitted yield $N(B_s^0 \to \eta'\phi)$ and on the yield ratio $R = N(B_s^0 \to \eta'\phi)/N(B^+ \to \eta' K^+)$, respectively. The last line gives the quadratic sum of the individual uncertainties.

with the systematic uncertainties, and α is the confidence level (CL). The obtained upper limits are

$$N(B_s^0 \to \eta'\phi) < 8.9\ (10.9) \qquad \text{at} \quad 90\%\ (95\%)\ \text{CL}$$

and

$$\frac{N(B_s^0 \to \eta'\phi)}{N(B^+ \to \eta' K^+)} < 8.0\ (9.9) \times 10^{-4} \qquad \text{at} \quad 90\%\ (95\%)\ \text{CL}\,.$$

5 Result and conclusion

A search has been performed for the $B_s^0 \to \eta'\phi$ decay. No signal is found. The branching fraction $\mathcal{B}(B_s^0 \to \eta'\phi) = (-0.18^{+0.47}_{-0.36}(\text{stat}) \pm 0.10(\text{syst})) \times 10^{-6}$ is computed from eqs. (1.1), (3.1) and (4.2) using the known value of $\mathcal{B}(B^+ \to \eta' K^+)$ [10] and the LHCb measurement of f_s/f_d [11, 12], which leads to

$$\mathcal{B}(B_s^0 \to \eta'\phi) < 0.82\,(1.01) \times 10^{-6} \qquad \text{at} \quad 90\%\ (95\%)\ \text{CL}$$

using the likelihood integration method described above. This is the first upper limit set on the $B_s^0 \to \eta'\phi$ branching fraction.

This result favours the lower end of the range of predictions for this branching fraction, pointing to form factors consistent with the light-cone sum-rule calculation used in ref. [4], or with the hypotheses used in refs. [3, 5]. Although large theoretical uncertainties make most predictions compatible with the result of this analysis, the central values of the predictions in refs. [6–9] are significantly larger than the upper limit. These discrepancies should help in constraining the theoretical models used in the prediction of branching fractions and *CP* asymmetries for B-meson hadronic charmless decays.

Acknowledgments

We express our gratitude to our colleagues in the CERN accelerator departments for the excellent performance of the LHC. We thank the technical and administrative staff at the LHCb institutes. We acknowledge support from CERN and from the national agencies: CAPES, CNPq, FAPERJ and FINEP (Brazil); NSFC (China); CNRS/IN2P3

JHEP05(2017)158

(France); BMBF, DFG and MPG (Germany); INFN (Italy); FOM and NWO (The Netherlands); MNiSW and NCN (Poland); MEN/IFA (Romania); MinES and FASO (Russia); MinECo (Spain); SNSF and SER (Switzerland); NASU (Ukraine); STFC (United Kingdom); NSF (U.S.A.). We acknowledge the computing resources that are provided by CERN, IN2P3 (France), KIT and DESY (Germany), INFN (Italy), SURF (The Netherlands), PIC (Spain), GridPP (United Kingdom), RRCKI and Yandex LLC (Russia), CSCS (Switzerland), IFIN-HH (Romania), CBPF (Brazil), PL-GRID (Poland) and OSC (U.S.A.). We are indebted to the communities behind the multiple open source software packages on which we depend. Individual groups or members have received support from AvH Foundation (Germany), EPLANET, Marie Skłodowska-Curie Actions and ERC (European Union), Conseil Général de Haute-Savoie, Labex ENIGMASS and OCEVU, Région Auvergne (France), RFBR and Yandex LLC (Russia), GVA, XuntaGal and GENCAT (Spain), Herchel Smith Fund, The Royal Society, Royal Commission for the Exhibition of 1851 and the Leverhulme Trust (United Kingdom).

References

[1] D. Zhang, Z.-j. Xiao and C.S. Li, *Branching ratios and CP-violating asymmetries of $B_s \to h_1 h_2$ decays in the general two Higgs doublet model*, *Phys. Rev.* **D 64** (2001) 014014 [hep-ph/0012063] [INSPIRE].

[2] LHCb collaboration, *Observation of the $B_s^0 \to \eta' \eta'$ decay*, *Phys. Rev. Lett.* **115** (2015) 051801 [arXiv:1503.07483] [INSPIRE].

[3] M. Beneke and M. Neubert, *QCD factorization for $B \to PP$ and $B \to PV$ decays*, *Nucl. Phys.* **B 675** (2003) 333 [hep-ph/0308039] [INSPIRE].

[4] H.-Y. Cheng and C.-K. Chua, *QCD Factorization for Charmless Hadronic B_s Decays Revisited*, *Phys. Rev.* **D 80** (2009) 114026 [arXiv:0910.5237] [INSPIRE].

[5] A. Ali et al., *Charmless non-leptonic B_s decays to PP, PV and VV final states in the pQCD approach*, *Phys. Rev.* **D 76** (2007) 074018 [hep-ph/0703162] [INSPIRE].

[6] X.-f. Chen, D.-q. Guo and Z.-j. Xiao, *$B_s^0 \to (\rho, \omega, \phi)\eta^{(\prime)}$ Decays in the Perturbative QCD Approach*, hep-ph/0701146 [INSPIRE].

[7] W. Wang, Y.-M. Wang, D.-S. Yang and C.-D. Lü, *Charmless Two-body $B_{(s)} \to VP$ decays In Soft-Collinear-Effective-Theory*, *Phys. Rev.* **D 78** (2008) 034011 [arXiv:0801.3123] [INSPIRE].

[8] H.-Y. Cheng, C.-W. Chiang and A.-L. Kuo, *Updating $B \to PP, VP$ decays in the framework of flavor symmetry*, *Phys. Rev.* **D 91** (2015) 014011 [arXiv:1409.5026] [INSPIRE].

[9] S.-H. Zhou, Q.-A. Zhang, W.-R. Lyu and C.-D. Lü, *Analysis of Charmless Two-body B decays in Factorization Assisted Topological Amplitude Approach*, *Eur. Phys. J.* **C 77** (2017) 125 [arXiv:1608.02819] [INSPIRE].

JHEP05(2017)158

[10] Particle Data Group collaboration, C. Patrignani et al., *Review of Particle Physics*, *Chin. Phys.* **C 40** (2016) 100001 [INSPIRE].

[11] LHCb collaboration, *Measurement of the fragmentation fraction ratio f_s/f_d and its dependence on B meson kinematics*, *JHEP* **04** (2013) 001 [arXiv:1301.5286] [INSPIRE].

[12] LHCb collaboration, *Updated average f_s/f_d b-hadron production fraction ratio for 7 TeV pp collisions*, LHCb-CONF-2013-011 (2013) [INSPIRE].

[13] LHCb collaboration, *The LHCb Detector at the LHC*, 2008 *JINST* **3** S08005 [INSPIRE].

[14] LHCb collaboration, *LHCb Detector Performance*, *Int. J. Mod. Phys.* **A 30** (2015) 1530022 [arXiv:1412.6352] [INSPIRE].

[15] R. Aaij et al., *The LHCb Trigger and its Performance in 2011*, 2013 *JINST* **8** P04022 [arXiv:1211.3055] [INSPIRE].

[16] V.V. Gligorov and M. Williams, *Efficient, reliable and fast high-level triggering using a bonsai boosted decision tree*, 2013 *JINST* **8** P02013 [arXiv:1210.6861] [INSPIRE].

[17] T. Sjöstrand, S. Mrenna and P.Z. Skands, *PYTHIA 6.4 Physics and Manual*, *JHEP* **05** (2006) 026 [hep-ph/0603175] [INSPIRE].

[18] T. Sjöstrand, S. Mrenna and P.Z. Skands, *A Brief Introduction to PYTHIA 8.1*, *Comput. Phys. Commun.* **178** (2008) 852 [arXiv:0710.3820] [INSPIRE].

[19] LHCb collaboration, *Handling of the generation of primary events in Gauss, the LHCb simulation framework*, *J. Phys. Conf. Ser.* **331** (2011) 032047 [INSPIRE].

[20] D.J. Lange, *The EvtGen particle decay simulation package*, *Nucl. Instrum. Meth.* **A 462** (2001) 152 [INSPIRE].

[21] P. Golonka and Z. Was, *PHOTOS Monte Carlo: A Precision tool for QED corrections in Z and W decays*, *Eur. Phys. J.* **C 45** (2006) 97 [hep-ph/0506026] [INSPIRE].

[22] Geant4 collaboration, J. Allison et al., *Geant4 developments and applications*, *IEEE Trans. Nucl. Sci.* **53** (2006) 270 [INSPIRE].

[23] Geant4 collaboration, S. Agostinelli et al., *GEANT4: A Simulation toolkit*, *Nucl. Instrum. Meth.* **A 506** (2003) 250 [INSPIRE].

[24] LHCb collaboration, *The LHCb simulation application, Gauss: Design, evolution and experience*, *J. Phys. Conf. Ser.* **331** (2011) 032023 [INSPIRE].

[25] L. Breiman, J.H. Friedman, R.A. Olshen and C.J. Stone, *Classification and regression trees*, Wadsworth international group, Belmont California U.S.A. (1984).

[26] Y. Freund and R.E. Schapire, *A decision-theoretic generalization of on-line learning and an application to boosting*, *J. Comput. Syst. Sci.* **55** (1997) 119 [INSPIRE].

[27] A. Blum, A. Kalai and J. Langford, *Beating the hold-out: Bounds for k-fold and progressive cross-validation*, in proceedings of the *Twelfth Annual Conference on Computational Learning Theory (COLT '99)*, Santa Cruz, California, U.S.A., 7–9 July 1999, ACM, New York NY U.S.A. (1999), p. 203.

[28] G. Punzi, *Sensitivity of searches for new signals and its optimization*, in *Statistical Problems in Particle Physics, Astrophysics, and Cosmology*, L. Lyons, R. Mount and R. Reitmeyer eds., SLAC, Menlo Park California U.S.A. (2003), p. 79 [*eConf* **C 030908** (2003) MODT002] [physics/0308063] [INSPIRE].

JHEP05(2017)158

[29] S.S. Wilks, *The large-sample distribution of the likelihood ratio for testing composite hypotheses*, *Annals Math. Statist.* **9** (1938) 60 [INSPIRE].

[30] M. Pivk and F.R. Le Diberder, *SPlot: A Statistical tool to unfold data distributions*, *Nucl. Instrum. Meth.* **A 555** (2005) 356 [physics/0402083] [INSPIRE].

[31] M. Adinolfi et al., *Performance of the LHCb RICH detector at the LHC*, *Eur. Phys. J.* **C 73** (2013) 2431 [arXiv:1211.6759] [INSPIRE].

[32] LHCb collaboration, *Measurement of the track reconstruction efficiency at LHCb*, 2015 *JINST* **10** P02007 [arXiv:1408.1251] [INSPIRE].

[33] K.S. Cranmer, *Kernel estimation in high-energy physics*, *Comput. Phys. Commun.* **136** (2001) 198 [hep-ex/0011057] [INSPIRE].

JHEP05(2017)158

The LHCb collaboration

R. Aaij[40], B. Adeva[39], M. Adinolfi[48], Z. Ajaltouni[5], S. Akar[59], J. Albrecht[10], F. Alessio[40], M. Alexander[53], S. Ali[43], G. Alkhazov[31], P. Alvarez Cartelle[55], A.A. Alves Jr[59], S. Amato[2], S. Amerio[23], Y. Amhis[7], L. An[3], L. Anderlini[18], G. Andreassi[41], M. Andreotti[17,g], J.E. Andrews[60], R.B. Appleby[56], F. Archilli[43], P. d'Argent[12], J. Arnau Romeu[6], A. Artamonov[37], M. Artuso[61], E. Aslanides[6], G. Auriemma[26], M. Baalouch[5], I. Babuschkin[56], S. Bachmann[12], J.J. Back[50], A. Badalov[38], C. Baesso[62], S. Baker[55], V. Balagura[7,c], W. Baldini[17], R.J. Barlow[56], C. Barschel[40], S. Barsuk[7], W. Barter[56], F. Baryshnikov[32], M. Baszczyk[27], V. Batozskaya[29], B. Batsukh[61], V. Battista[41], A. Bay[41], L. Beaucourt[4], J. Beddow[53], F. Bedeschi[24], I. Bediaga[1], L.J. Bel[43], V. Bellee[41], N. Belloli[21,i], K. Belous[37], I. Belyaev[32], E. Ben-Haim[8], G. Bencivenni[19], S. Benson[43], A. Berezhnoy[33], R. Bernet[42], A. Bertolin[23], C. Betancourt[42], F. Betti[15], M.-O. Bettler[40], M. van Beuzekom[43], Ia. Bezshyiko[42], S. Bifani[47], P. Billoir[8], T. Bird[56], A. Birnkraut[10], A. Bitadze[56], A. Bizzeti[18,u], T. Blake[50], F. Blanc[41], J. Blouw[11,†], S. Blusk[61], V. Bocci[26], T. Boettcher[58], A. Bondar[36,w], N. Bondar[31,40], W. Bonivento[16], I. Bordyuzhin[32], A. Borgheresi[21,i], S. Borghi[56], M. Borisyak[35], M. Borsato[39], F. Bossu[7], M. Boubdir[9], T.J.V. Bowcock[54], E. Bowen[42], C. Bozzi[17,40], S. Braun[12], M. Britsch[12], T. Britton[61], J. Brodzicka[56], E. Buchanan[48], C. Burr[56], A. Bursche[2], J. Buytaert[40], S. Cadeddu[16], R. Calabrese[17,g], M. Calvi[21,i], M. Calvo Gomez[38,m], A. Camboni[38], P. Campana[19], D.H. Campora Perez[40], L. Capriotti[56], A. Carbone[15,e], G. Carboni[25,j], R. Cardinale[20,h], A. Cardini[16], P. Carniti[21,i], L. Carson[52], K. Carvalho Akiba[2], G. Casse[54], L. Cassina[21,i], L. Castillo Garcia[41], M. Cattaneo[40], G. Cavallero[20], R. Cenci[24,t], D. Chamont[7], M. Charles[8], Ph. Charpentier[40], G. Chatzikonstantinidis[47], M. Chefdeville[4], S. Chen[56], S.-F. Cheung[57], V. Chobanova[39], M. Chrzaszcz[42,27], X. Cid Vidal[39], G. Ciezarek[43], P.E.L. Clarke[52], M. Clemencic[40], H.V. Cliff[49], J. Closier[40], V. Coco[59], J. Cogan[6], E. Cogneras[5], V. Cogoni[16,40,f], L. Cojocariu[30], G. Collazuol[23,o], P. Collins[40], A. Comerma-Montells[12], A. Contu[40], A. Cook[48], G. Coombs[40], S. Coquereau[38], G. Corti[40], M. Corvo[17,g], C.M. Costa Sobral[50], B. Couturier[40], G.A. Cowan[52], D.C. Craik[52], A. Crocombe[50], M. Cruz Torres[62], S. Cunliffe[55], R. Currie[55], C. D'Ambrosio[40], F. Da Cunha Marinho[2], E. Dall'Occo[43], J. Dalseno[48], P.N.Y. David[43], A. Davis[3], K. De Bruyn[6], S. De Capua[56], M. De Cian[12], J.M. De Miranda[1], L. De Paula[2], M. De Serio[14,d], P. De Simone[19], C.-T. Dean[53], D. Decamp[4], M. Deckenhoff[10], L. Del Buono[8], M. Demmer[10], A. Dendek[28], D. Derkach[35], O. Deschamps[5], F. Dettori[40], B. Dey[22], A. Di Canto[40], H. Dijkstra[40], F. Dordei[40], M. Dorigo[41], A. Dosil Suárez[39], A. Dovbnya[45], K. Dreimanis[54], L. Dufour[43], G. Dujany[56], K. Dungs[40], P. Durante[40], R. Dzhelyadin[37], A. Dziurda[40], A. Dzyuba[31], N. Déléage[4], S. Easo[51], M. Ebert[52], U. Egede[55], V. Egorychev[32], S. Eidelman[36,w], S. Eisenhardt[52], U. Eitschberger[10], R. Ekelhof[10], L. Eklund[53], S. Ely[61], S. Esen[12], H.M. Evans[49], T. Evans[57], A. Falabella[15], N. Farley[47], S. Farry[54], R. Fay[54], D. Fazzini[21,i], D. Ferguson[52], A. Fernandez Prieto[39], F. Ferrari[15,40], F. Ferreira Rodrigues[2], M. Ferro-Luzzi[40], S. Filippov[34], R.A. Fini[14], M. Fiore[17,g], M. Fiorini[17,g], M. Firlej[28], C. Fitzpatrick[41], T. Fiutowski[28], F. Fleuret[7,b], K. Fohl[40], M. Fontana[16,40], F. Fontanelli[20,h], D.C. Forshaw[61], R. Forty[40], V. Franco Lima[54], M. Frank[40], C. Frei[40], J. Fu[22,q], W. Funk[40], E. Furfaro[25,j], C. Färber[40], A. Gallas Torreira[39], D. Galli[15,e], S. Gallorini[23], S. Gambetta[52], M. Gandelman[2], P. Gandini[57], Y. Gao[3], L.M. Garcia Martin[69], J. García Pardiñas[39], J. Garra Tico[49], L. Garrido[38], P.J. Garsed[49], D. Gascon[38], C. Gaspar[40], L. Gavardi[10], G. Gazzoni[5], D. Gerick[12], E. Gersabeck[12], M. Gersabeck[56], T. Gershon[50], Ph. Ghez[4], S. Gianì[41], V. Gibson[49], O.G. Girard[41], L. Giubega[30], K. Gizdov[52], V.V. Gligorov[8], D. Golubkov[32], A. Golutvin[55,40], A. Gomes[1,a], I.V. Gorelov[33], C. Gotti[21,i], R. Graciani Diaz[38], L.A. Granado Cardoso[40], E. Graugés[38], E. Graverini[42], G. Graziani[18], A. Grecu[30], P. Griffith[47], L. Grillo[21,40,i], B.R. Gruberg Cazon[57], O. Grünberg[67], E. Gushchin[34], Yu. Guz[37], T. Gys[40], C. Göbel[62], T. Hadavizadeh[57], C. Hadjivasiliou[5], G. Haefeli[41], C. Haen[40], S.C. Haines[49], B. Hamilton[60], X. Han[12], S. Hansmann-Menzemer[12],

JHEP05(2017)158

N. Harnew[57], S.T. Harnew[48], J. Harrison[56], M. Hatch[40], J. He[63], T. Head[41], A. Heister[9], K. Hennessy[54], P. Henrard[5], L. Henry[8], E. van Herwijnen[40], M. Heß[67], A. Hicheur[2], D. Hill[57], C. Hombach[56], H. Hopchev[41], W. Hulsbergen[43], T. Humair[55], M. Hushchyn[35], D. Hutchcroft[54], M. Idzik[28], P. Ilten[58], R. Jacobsson[40], A. Jaeger[12], J. Jalocha[57], E. Jans[43], A. Jawahery[60], F. Jiang[3], M. John[57], D. Johnson[40], C.R. Jones[49], C. Joram[40], B. Jost[40], N. Jurik[57], S. Kandybei[45], M. Karacson[40], J.M. Kariuki[48], S. Karodia[53], M. Kecke[12], M. Kelsey[61], M. Kenzie[49], T. Ketel[44], E. Khairullin[35], B. Khanji[12], C. Khurewathanakul[41], T. Kirn[9], S. Klaver[56], K. Klimaszewski[29], S. Koliiev[46], M. Kolpin[12], I. Komarov[41], R.F. Koopman[44], P. Koppenburg[43], A. Kosmyntseva[32], A. Kozachuk[33], M. Kozeiha[5], L. Kravchuk[34], K. Kreplin[12], M. Kreps[50], P. Krokovny[36,w], F. Kruse[10], W. Krzemien[29], W. Kucewicz[27,l], M. Kucharczyk[27], V. Kudryavtsev[36,w], A.K. Kuonen[41], K. Kurek[29], T. Kvaratskheliya[32,40], D. Lacarrere[40], G. Lafferty[56], A. Lai[16], G. Lanfranchi[19], C. Langenbruch[9], T. Latham[50], C. Lazzeroni[47], R. Le Gac[6], J. van Leerdam[43], A. Leflat[33,40], J. Lefrançois[7], R. Lefèvre[5], F. Lemaitre[40], E. Lemos Cid[39], O. Leroy[6], T. Lesiak[27], B. Leverington[12], T. Li[3], Y. Li[7], T. Likhomanenko[35,68], R. Lindner[40], C. Linn[40], F. Lionetto[42], X. Liu[3], D. Loh[50], I. Longstaff[53], J.H. Lopes[2], D. Lucchesi[23,o], M. Lucio Martinez[39], H. Luo[52], A. Lupato[23], E. Luppi[17,g], O. Lupton[40], A. Lusiani[24], X. Lyu[63], F. Machefert[7], F. Maciuc[30], O. Maev[31], K. Maguire[56], S. Malde[57], A. Malinin[68], T. Maltsev[36], G. Manca[16,f], G. Mancinelli[6], P. Manning[61], J. Maratas[5,v], J.F. Marchand[4], U. Marconi[15], C. Marin Benito[38], M. Marinangeli[41], P. Marino[24,t], J. Marks[12], G. Martellotti[26], M. Martin[6], M. Martinelli[41], D. Martinez Santos[39], F. Martinez Vidal[69], D. Martins Tostes[2], L.M. Massacrier[7], A. Massafferri[1], R. Matev[40], A. Mathad[50], Z. Mathe[40], C. Matteuzzi[21], A. Mauri[42], E. Maurice[7,b], B. Maurin[41], A. Mazurov[47], M. McCann[55,40], A. McNab[56], R. McNulty[13], B. Meadows[59], F. Meier[10], M. Meissner[12], D. Melnychuk[29], M. Merk[43], A. Merli[22,q], E. Michielin[23], D.A. Milanes[66], M.-N. Minard[4], D.S. Mitzel[12], A. Mogini[8], J. Molina Rodriguez[1], I.A. Monroy[66], S. Monteil[5], M. Morandin[23], P. Morawski[28], A. Mordà[6], M.J. Morello[24,t], O. Morgunova[68], J. Moron[28], A.B. Morris[52], R. Mountain[61], F. Muheim[52], M. Mulder[43], M. Mussini[15], D. Müller[56], J. Müller[10], K. Müller[42], V. Müller[10], P. Naik[48], T. Nakada[41], R. Nandakumar[51], A. Nandi[57], I. Nasteva[2], M. Needham[52], N. Neri[22], S. Neubert[12], N. Neufeld[40], M. Neuner[12], T.D. Nguyen[41], C. Nguyen-Mau[41,n], S. Nieswand[9], R. Niet[10], N. Nikitin[33], T. Nikodem[12], A. Nogay[68], A. Novoselov[37], D.P. O'Hanlon[50], A. Oblakowska-Mucha[28], V. Obraztsov[37], S. Ogilvy[19], R. Oldeman[16,f], C.J.G. Onderwater[70], J.M. Otalora Goicochea[2], A. Otto[40], P. Owen[42], A. Oyanguren[69], P.R. Pais[41], A. Palano[14,d], M. Palutan[19], A. Papanestis[51], M. Pappagallo[14,d], L.L. Pappalardo[17,g], W. Parker[60], C. Parkes[56], G. Passaleva[18], A. Pastore[14,d], G.D. Patel[54], M. Patel[55], C. Patrignani[15,e], A. Pearce[40], A. Pellegrino[43], G. Penso[26], M. Pepe Altarelli[40], S. Perazzini[40], P. Perret[5], L. Pescatore[47], K. Petridis[48], A. Petrolini[20,h], A. Petrov[68], M. Petruzzo[22,q], E. Picatoste Olloqui[38], B. Pietrzyk[4], M. Pikies[27], D. Pinci[26], A. Pistone[20], A. Piucci[12], V. Placinta[30], S. Playfer[52], M. Plo Casasus[39], T. Poikela[40], F. Polci[8], A. Poluektov[50,36], I. Polyakov[61], E. Polycarpo[2], G.J. Pomery[48], A. Popov[37], D. Popov[11,40], B. Popovici[30], S. Poslavskii[37], C. Potterat[2], E. Price[48], J.D. Price[54], J. Prisciandaro[39,40], A. Pritchard[54], C. Prouve[48], V. Pugatch[46], A. Puig Navarro[42], G. Punzi[24,p], W. Qian[50], R. Quagliani[7,48], B. Rachwal[27], J.H. Rademacker[48], M. Rama[24], M. Ramos Pernas[39], M.S. Rangel[2], I. Raniuk[45], F. Ratnikov[35], G. Raven[44], F. Redi[55], S. Reichert[10], A.C. dos Reis[1], C. Remon Alepuz[69], V. Renaudin[7], S. Ricciardi[51], S. Richards[48], M. Rihl[40], K. Rinnert[54], V. Rives Molina[38], P. Robbe[7,40], A.B. Rodrigues[1], E. Rodrigues[59], J.A. Rodriguez Lopez[66], P. Rodriguez Perez[56,†], A. Rogozhnikov[35], S. Roiser[40], A. Rollings[57], V. Romanovskiy[37], A. Romero Vidal[39], J.W. Ronayne[13], M. Rotondo[19], M.S. Rudolph[61], T. Ruf[40], P. Ruiz Valls[69], J.J. Saborido Silva[39], E. Sadykhov[32], N. Sagidova[31], B. Saitta[16,f], V. Salustino Guimaraes[1], C. Sanchez Mayordomo[69], B. Sanmartin Sedes[39], R. Santacesaria[26], C. Santamarina Rios[39], M. Santimaria[19], E. Santovetti[25,j], A. Sarti[19,k], C. Satriano[26,s], A. Satta[25], D.M. Saunders[48],

JHEP05(2017)158

D. Savrina[32,33], S. Schael[9], M. Schellenberg[10], M. Schiller[53], H. Schindler[40], M. Schlupp[10], M. Schmelling[11], T. Schmelzer[10], B. Schmidt[40], O. Schneider[41], A. Schopper[40], K. Schubert[10], M. Schubiger[41], M.-H. Schune[7], R. Schwemmer[40], B. Sciascia[19], A. Sciubba[26,k], A. Semennikov[32], A. Sergi[47], N. Serra[42], J. Serrano[6], L. Sestini[23], P. Seyfert[21], M. Shapkin[37], I. Shapoval[45], Y. Shcheglov[31], T. Shears[54], L. Shekhtman[36,w], V. Shevchenko[68], B.G. Siddi[17,40], R. Silva Coutinho[42], L. Silva de Oliveira[2], G. Simi[23,o], S. Simone[14,d], M. Sirendi[49], N. Skidmore[48], T. Skwarnicki[61], E. Smith[55], I.T. Smith[52], J. Smith[49], M. Smith[55], H. Snoek[43], l. Soares Lavra[1], M.D. Sokoloff[59], F.J.P. Soler[53], B. Souza De Paula[2], B. Spaan[10], P. Spradlin[53], S. Sridharan[40], F. Stagni[40], M. Stahl[12], S. Stahl[40], P. Stefko[41], S. Stefkova[55], O. Steinkamp[42], S. Stemmle[12], O. Stenyakin[37], H. Stevens[10], S. Stevenson[57], S. Stoica[30], S. Stone[61], B. Storaci[42], S. Stracka[24,p], M. Straticiuc[30], U. Straumann[42], L. Sun[64], W. Sutcliffe[55], K. Swientek[28], V. Syropoulos[44], M. Szczekowski[29], T. Szumlak[28], S. T'Jampens[4], A. Tayduganov[6], T. Tekampe[10], G. Tellarini[17,g], F. Teubert[40], E. Thomas[40], J. van Tilburg[43], M.J. Tilley[55], V. Tisserand[4], M. Tobin[41], S. Tolk[49], L. Tomassetti[17,g], D. Tonelli[40], S. Topp-Joergensen[57], F. Toriello[61], E. Tournefier[4], S. Tourneur[41], K. Trabelsi[41], M. Traill[53], M.T. Tran[41], M. Tresch[42], A. Trisovic[40], A. Tsaregorodtsev[6], P. Tsopelas[43], A. Tully[49], N. Tuning[43], A. Ukleja[29], A. Ustyuzhanin[35], U. Uwer[12], C. Vacca[16,f], V. Vagnoni[15,40], A. Valassi[40], S. Valat[40], G. Valenti[15], R. Vazquez Gomez[19], P. Vazquez Regueiro[39], S. Vecchi[17], M. van Veghel[43], J.J. Velthuis[48], M. Veltri[18,r], G. Veneziano[57], A. Venkateswaran[61], M. Vernet[5], M. Vesterinen[12], J.V. Viana Barbosa[40], B. Viaud[7], D. Vieira[63], M. Vieites Diaz[39], H. Viemann[67], X. Vilasis-Cardona[38,m], M. Vitti[49], V. Volkov[33], A. Vollhardt[42], B. Voneki[40], A. Vorobyev[31], V. Vorobyev[36,w], C. Voß[9], J.A. de Vries[43], C. Vázquez Sierra[39], R. Waldi[67], C. Wallace[50], R. Wallace[13], J. Walsh[24], J. Wang[61], D.R. Ward[49], H.M. Wark[54], N.K. Watson[47], D. Websdale[55], A. Weiden[42], M. Whitehead[40], J. Wicht[50], G. Wilkinson[57,40], M. Wilkinson[61], M. Williams[40], M.P. Williams[47], M. Williams[58], T. Williams[47], F.F. Wilson[51], J. Wimberley[60], J. Wishahi[10], W. Wislicki[29], M. Witek[27], G. Wormser[7], S.A. Wotton[49], K. Wraight[53], K. Wyllie[40], Y. Xie[65], Z. Xing[61], Z. Xu[4], Z. Yang[3], Y. Yao[61], H. Yin[65], J. Yu[65], X. Yuan[36,w], O. Yushchenko[37], K.A. Zarebski[47], M. Zavertyaev[11,c], L. Zhang[3], Y. Zhang[7], Y. Zhang[63], A. Zhelezov[12], Y. Zheng[63], X. Zhu[3], V. Zhukov[33], S. Zucchelli[15].

[1] *Centro Brasileiro de Pesquisas Físicas (CBPF), Rio de Janeiro, Brazil*
[2] *Universidade Federal do Rio de Janeiro (UFRJ), Rio de Janeiro, Brazil*
[3] *Center for High Energy Physics, Tsinghua University, Beijing, China*
[4] *LAPP, Université Savoie Mont-Blanc, CNRS/IN2P3, Annecy-Le-Vieux, France*
[5] *Clermont Université, Université Blaise Pascal, CNRS/IN2P3, LPC, Clermont-Ferrand, France*
[6] *CPPM, Aix-Marseille Université, CNRS/IN2P3, Marseille, France*
[7] *LAL, Université Paris-Sud, CNRS/IN2P3, Orsay, France*
[8] *LPNHE, Université Pierre et Marie Curie, Université Paris Diderot, CNRS/IN2P3, Paris, France*
[9] *I. Physikalisches Institut, RWTH Aachen University, Aachen, Germany*
[10] *Fakultät Physik, Technische Universität Dortmund, Dortmund, Germany*
[11] *Max-Planck-Institut für Kernphysik (MPIK), Heidelberg, Germany*
[12] *Physikalisches Institut, Ruprecht-Karls-Universität Heidelberg, Heidelberg, Germany*
[13] *School of Physics, University College Dublin, Dublin, Ireland*
[14] *Sezione INFN di Bari, Bari, Italy*
[15] *Sezione INFN di Bologna, Bologna, Italy*
[16] *Sezione INFN di Cagliari, Cagliari, Italy*
[17] *Sezione INFN di Ferrara, Ferrara, Italy*
[18] *Sezione INFN di Firenze, Firenze, Italy*
[19] *Laboratori Nazionali dell'INFN di Frascati, Frascati, Italy*
[20] *Sezione INFN di Genova, Genova, Italy*
[21] *Sezione INFN di Milano Bicocca, Milano, Italy*

JHEP05(2017)158

[22] Sezione INFN di Milano, Milano, Italy
[23] Sezione INFN di Padova, Padova, Italy
[24] Sezione INFN di Pisa, Pisa, Italy
[25] Sezione INFN di Roma Tor Vergata, Roma, Italy
[26] Sezione INFN di Roma La Sapienza, Roma, Italy
[27] Henryk Niewodniczanski Institute of Nuclear Physics Polish Academy of Sciences, Kraków, Poland
[28] AGH - University of Science and Technology, Faculty of Physics and Applied Computer Science, Kraków, Poland
[29] National Center for Nuclear Research (NCBJ), Warsaw, Poland
[30] Horia Hulubei National Institute of Physics and Nuclear Engineering, Bucharest-Magurele, Romania
[31] Petersburg Nuclear Physics Institute (PNPI), Gatchina, Russia
[32] Institute of Theoretical and Experimental Physics (ITEP), Moscow, Russia
[33] Institute of Nuclear Physics, Moscow State University (SINP MSU), Moscow, Russia
[34] Institute for Nuclear Research of the Russian Academy of Sciences (INR RAN), Moscow, Russia
[35] Yandex School of Data Analysis, Moscow, Russia
[36] Budker Institute of Nuclear Physics (SB RAS), Novosibirsk, Russia
[37] Institute for High Energy Physics (IHEP), Protvino, Russia
[38] ICCUB, Universitat de Barcelona, Barcelona, Spain
[39] Universidad de Santiago de Compostela, Santiago de Compostela, Spain
[40] European Organization for Nuclear Research (CERN), Geneva, Switzerland
[41] Institute of Physics, Ecole Polytechnique Fédérale de Lausanne (EPFL), Lausanne, Switzerland
[42] Physik-Institut, Universität Zürich, Zürich, Switzerland
[43] Nikhef National Institute for Subatomic Physics, Amsterdam, The Netherlands
[44] Nikhef National Institute for Subatomic Physics and VU University Amsterdam, Amsterdam, The Netherlands
[45] NSC Kharkiv Institute of Physics and Technology (NSC KIPT), Kharkiv, Ukraine
[46] Institute for Nuclear Research of the National Academy of Sciences (KINR), Kyiv, Ukraine
[47] University of Birmingham, Birmingham, United Kingdom
[48] H.H. Wills Physics Laboratory, University of Bristol, Bristol, United Kingdom
[49] Cavendish Laboratory, University of Cambridge, Cambridge, United Kingdom
[50] Department of Physics, University of Warwick, Coventry, United Kingdom
[51] STFC Rutherford Appleton Laboratory, Didcot, United Kingdom
[52] School of Physics and Astronomy, University of Edinburgh, Edinburgh, United Kingdom
[53] School of Physics and Astronomy, University of Glasgow, Glasgow, United Kingdom
[54] Oliver Lodge Laboratory, University of Liverpool, Liverpool, United Kingdom
[55] Imperial College London, London, United Kingdom
[56] School of Physics and Astronomy, University of Manchester, Manchester, United Kingdom
[57] Department of Physics, University of Oxford, Oxford, United Kingdom
[58] Massachusetts Institute of Technology, Cambridge, MA, United States
[59] University of Cincinnati, Cincinnati, OH, United States
[60] University of Maryland, College Park, MD, United States
[61] Syracuse University, Syracuse, NY, United States
[62] Pontifícia Universidade Católica do Rio de Janeiro (PUC-Rio), Rio de Janeiro, Brazil, associated to [2]
[63] University of Chinese Academy of Sciences, Beijing, China, associated to [3]
[64] School of Physics and Technology, Wuhan University, Wuhan, China, associated to [3]
[65] Institute of Particle Physics, Central China Normal University, Wuhan, Hubei, China, associated to [3]
[66] Departamento de Fisica , Universidad Nacional de Colombia, Bogota, Colombia, associated to [8]
[67] Institut für Physik, Universität Rostock, Rostock, Germany, associated to [12]

JHEP05(2017)158

[68] National Research Centre Kurchatov Institute, Moscow, Russia, associated to [32]
[69] Instituto de Fisica Corpuscular (IFIC), Universitat de Valencia-CSIC, Valencia, Spain, associated to [38]
[70] Van Swinderen Institute, University of Groningen, Groningen, The Netherlands, associated to [43]

[a] Universidade Federal do Triângulo Mineiro (UFTM), Uberaba-MG, Brazil
[b] Laboratoire Leprince-Ringuet, Palaiseau, France
[c] P.N. Lebedev Physical Institute, Russian Academy of Science (LPI RAS), Moscow, Russia
[d] Università di Bari, Bari, Italy
[e] Università di Bologna, Bologna, Italy
[f] Università di Cagliari, Cagliari, Italy
[g] Università di Ferrara, Ferrara, Italy
[h] Università di Genova, Genova, Italy
[i] Università di Milano Bicocca, Milano, Italy
[j] Università di Roma Tor Vergata, Roma, Italy
[k] Università di Roma La Sapienza, Roma, Italy
[l] AGH - University of Science and Technology, Faculty of Computer Science, Electronics and Telecommunications, Kraków, Poland
[m] LIFAELS, La Salle, Universitat Ramon Llull, Barcelona, Spain
[n] Hanoi University of Science, Hanoi, Viet Nam
[o] Università di Padova, Padova, Italy
[p] Università di Pisa, Pisa, Italy
[q] Università degli Studi di Milano, Milano, Italy
[r] Università di Urbino, Urbino, Italy
[s] Università della Basilicata, Potenza, Italy
[t] Scuola Normale Superiore, Pisa, Italy
[u] Università di Modena e Reggio Emilia, Modena, Italy
[v] Iligan Institute of Technology (IIT), Iligan, Philippines
[w] Novosibirsk State University, Novosibirsk, Russia

[†] Deceased

JHEP05(2017)158